

East Tennessee State University

## Digital Commons @ East Tennessee State University

---

Undergraduate Honors Theses

Student Works

---

5-2022

### Friedel-Crafts alkylation of benzene with a superacid catalyst

Josh T. Cutright

*East Tennessee State University*

Follow this and additional works at: <https://dc.etsu.edu/honors>

 Part of the [Organic Chemistry Commons](#)

---

#### Recommended Citation

Cutright, Josh T., "Friedel-Crafts alkylation of benzene with a superacid catalyst" (2022). *Undergraduate Honors Theses*. Paper 676. <https://dc.etsu.edu/honors/676>

This Honors Thesis - Open Access is brought to you for free and open access by the Student Works at Digital Commons @ East Tennessee State University. It has been accepted for inclusion in Undergraduate Honors Theses by an authorized administrator of Digital Commons @ East Tennessee State University. For more information, please contact [digilib@etsu.edu](mailto:digilib@etsu.edu).

Friedel-Crafts alkylation of benzene with a superacid catalyst

by

Josh Cutright

April 2022

---


An Undergraduate Thesis Submitted in Partial Fulfillment


of the Requirements for the

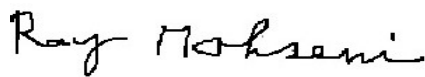
Honors-in-Discipline Program

East Tennessee State University

---

 5/4/22  
Josh Cutright Date

 05/04/2022  
Dr. Aleksey Vasiliev, Thesis Mentor Date



---

05/04/2022  
Dr. Ray Mohseni, Reader Date

## ABSTRACT

Long-chain alkylbenzenes are industrially synthesized precursors to commercial surfactants such as laundry detergent. The currently used catalysts in the processes of their synthesis are corrosive and harmful to the environment. These problems can be avoided utilizing heterogeneous highly acidic catalysts. Solid catalysts do not corrode equipment and are relatively simple to remove from the post-reaction mixture. Phosphotungstic acid (PTA) supported on silica gel could be a possible catalyst due to its high acidity with an estimated  $pK_a \approx -13$ . The catalyst PTA-SiO<sub>2</sub> was prepared via the sol-gel method to covalently embed it in a silica support. The catalyst was granulated with  $\gamma$ -alumina for use in a fixed bed flow reactor during the alkylation of benzene with long chain alkenes. The isomerization of 1-octene, 1-decene, and 1-octadecene as well as the conversion of 1-decene in the alkylation of benzene were studied under varying conditions. During these reactions, the catalyst demonstrated good catalytic activity at temperatures above 200 °C with an optimal temperature of 250 °C. Of all three alkenes, 1-octadecene showed the highest conversion into respective isomers. The alkylation of benzene with 1-decene experiments showed decreasing of flow rate and increasing the ratio of benzene to 1-decene lead to higher conversions of 1-decene. Characterization of the catalyst after the reaction showed little changes in porosity and particle size. No leaching of PTA was observed. However, carbon deposits were found on the catalyst that requires regeneration before next use in catalysis.

Copyright 2022 by Josh Cutright

All Rights Reserved

## DEDICATION

This work is dedicated to my friends and family.

## ACKNOWLEDGEMENTS

I would like to thank my research mentor Dr. Aleksey Vasiliev for his patience and guidance throughout this project. I would also like to thank him for the opportunity to work on this research.

I would also like to thank my reader Dr. Ray Mohseni, who also helped greatly in the instrumentation and analysis for the research.

I would like to thank Kofi Kankam and Anastasia Kuvayskaya, the previous graduate students who assisted with earlier projects in this research and who helped train me.

I want to also thank Robert Jauregui, Savana Edwards, and Jaykob Stephens, my fellow undergraduate students, for their assistance with experiments and analysis.

I want to thank Dr. Abbas Shilabin and Dr. Marina Roginskaya for their guidance through the Chemistry Honors-In-Discipline program.

I want to give a special thanks to the American Chemical Society Petroleum Research Fund for providing funds for the research (grant PRF # 58891-UR5).

## Table of Contents:

ABSTRACT.....	2
DEDICATION.....	4
ACKNOWLEDGMENTS.....	5
TABLE OF CONTENTS.....	6
LIST OF TABLES.....	8
LIST OF FIGURES.....	9
LIST OF ABBREVIATIONS.....	11
I. Introduction.....	12
1.1 Long Chain Alkylbenzenes.....	12
1.2 Heterogenous Catalysts.....	16
1.3 Heteropolyacids.....	19
1.4 Supported Heteropolyacids.....	21
1.5 Research Objectives .....	24
II. Experimental.....	25
2.1 Reagents and Materials.....	25
2.2 Catalyst Preparation.....	26
Sol-Gel Synthesis.....	26
Catalyst Pre-treatment.....	26
2.3 Instrumental Characterization.....	27
Elemental Analysis.....	27
Fourier-Transform Infrared Spectroscopy.....	27
Scanning Electron Microscopy.....	28

	BET Surface Area.....	28
	Particle Size Distribution.....	28
	Analysis of Reaction Mixtures.....	28
2.4	Catalytic Properties.....	29
	Isomerization of Alkenes .....	29
	Alkylation of Benzene .....	30
III.	Results and Discussion.....	31
3.1	Physical Characteristics and Chemical Composition.....	31
	Immobilized PTA-SiO <sub>2</sub> .....	31
	γ-Alumina Characteristics.....	34
	Granulated PTA-SiO <sub>2</sub> /Al <sub>2</sub> O <sub>3</sub> .....	34
3.2	Catalytic Activity.....	35
	Isomerization of Alkenes.....	35
	Alkylation of Benzene by 1-Decene.....	37
3.3	Deactivated Catalyst.....	42
	Chemical Composition.....	42
	Physical Characteristics.....	43
	CONCLUSIONS.....	44
	REFERENCES.....	45



## LIST OF TABLES

Table 1. Chemicals utilized.....	26
Table 2. Catalyst characteristics.....	32

## LIST OF FIGURES

Figure 1. Friedel Crafts alkylation of benzene mechanism.....	13
Figure 2. General structure of LAS ( $C_6H_4C_nH_{2n+1}SO_3Na$ ).....	14
Figure 3. Detal <sup>TM</sup> process flow scheme.....	16
Figure 4. Keggin structure $H_nXM_{12}O_{40}$ consisting of phosphorous (pink) as X, tungsten (blue) as M, oxygen (red) and hydrogen (white) .....	20
Figure 5. Sol-gel synthesis of PTA-SiO <sub>2</sub> catalyst.....	23
Figure 6. Carver 13 mm pellet die used to form tablets.....	27
Figure 7. Fixed bed flow reactor used in the isomerization of alkenes and alkylation of benzene reactions .....	30
Figure 8. FT-IR of the catalysts: PTA-SiO <sub>2</sub> (1), $\gamma$ -Al <sub>2</sub> O <sub>3</sub> (2), PTA-SiO <sub>2</sub> /Al <sub>2</sub> O <sub>3</sub> (3), and post-reaction PTA-SiO <sub>2</sub> /Al <sub>2</sub> O <sub>3</sub> .....	32
Figure 9. SEM image of PTA-SiO <sub>2</sub> .....	33
Figure 10. Particle size distribution (nm) for PTA-SiO <sub>2</sub> , $\gamma$ -Al <sub>2</sub> O <sub>3</sub> , fresh PTA-SiO <sub>2</sub> /Al <sub>2</sub> O <sub>3</sub> , and spent (post reaction) PTA-SiO <sub>2</sub> /Al <sub>2</sub> O <sub>3</sub> .....	33
Figure 11. GC-MS chromatograms of 1-octene (1), 1-decene (2), and 1-octadecene (3).....	35
Figure 12. Conversion of 1-octene (1), 1-decene (2), and 1-octadecene (3) into isomers.....	36
Figure 13. Alkylation of benzene with 1-decene and isomers formed.....	37
Figure 14. Reactant mixture of benzene (highest signal, 5.5 min.) and 1-decene (5.7 min.).....	38
Figure 15. Product mixture of benzene (5.5 min.), decene isomers (5.6-6.0 min.), and phenyldecane isomers (11.2-12.0 min.) .....	38
Figure 16. Phenyldecane isomers distribution .....	39
Figure 17. Effects of flow rate (left) and molar ratio (right) on the conversion of 1-decene .....	40

Figure 18. Conversion of 1-decene at various reaction temperatures.....42

## LIST OF ABBREVIATIONS

AAS	Atomic absorption spectroscopy
ARCO	Atlantic Richfield Company
BET	Brunauer-Emmett-Teller theory
DLS	Dynamic light scattering
FID	Flame ionization detector
FT-IR	Fourier-transform infrared spectroscopy
GC-MS	Gas chromatography with mass spectrometry detector
HPA	Heteropolyacid
HPMo	Molybdophosphoric acid
HSiW	Tungstosilic acid
LAB	Linear alkylbenzene
LAS	Linear alkylbenzene sulfonate
PDI	Polydispersity index
PTA	Phosphotungstic (tungstophosphoric) acid
SEM	Scanning electron microscopy
TEOS	Tetraethyl orthosilicate
UOP	Universal Oil Products
ZSM	Zeolite Socony Mobil

## I. Introduction

### 1.1 Long-Chain Alkylbenzenes

Long-chain alkylbenzenes, sometimes known as linear alkyl benzenes (LABs), are secondary C<sub>10-14</sub> substituted benzenes. These compounds are commonly synthesized through the Friedel Crafts alkylation in which an acid catalyst is used to protonate a long-chain alkene that will subsequently react and attach onto a benzene ideally at the second carbon in the chain (C2). The Friedel Crafts method is prone to hydride shifts on the protonated alkene chain resulted in a mixture of isomers as the product. The mechanism of this alkylation and hydride shift is shown in Figure 1. The process creates an intermediate compounds that can be further reacted to form useful products. Namely, LABs are important intermediates in the industrial production of linear alkylbenzene sulphonates (LAS). These products are utilized in a wide variety of fields including consumer use as laundry detergent and industrial use in textiles, polymers, pharmaceuticals, oil recovery, and even the paper industry<sup>1</sup>.

The LAS have been an essential product in many industries over the previous 45 years with an estimated two million tons of LAS consumed every year<sup>2</sup>. Much attention has been drawn to LAS due to the magnitude of its consumption and the poor effect on the environment. LAS life cycle includes the formulation production, use, and discharge of the LAS. The first two phases of the cycle produce very little waste as these phases occur in chemical plants where safe handling is common policy of waste materials. However, the mass of waste produced significantly increases during the later phases of the life cycle after they are used. It has been shown that LAS waste impairs organ functions in marine life and interferes with terrestrial invertebrate growth in soil<sup>3</sup>.

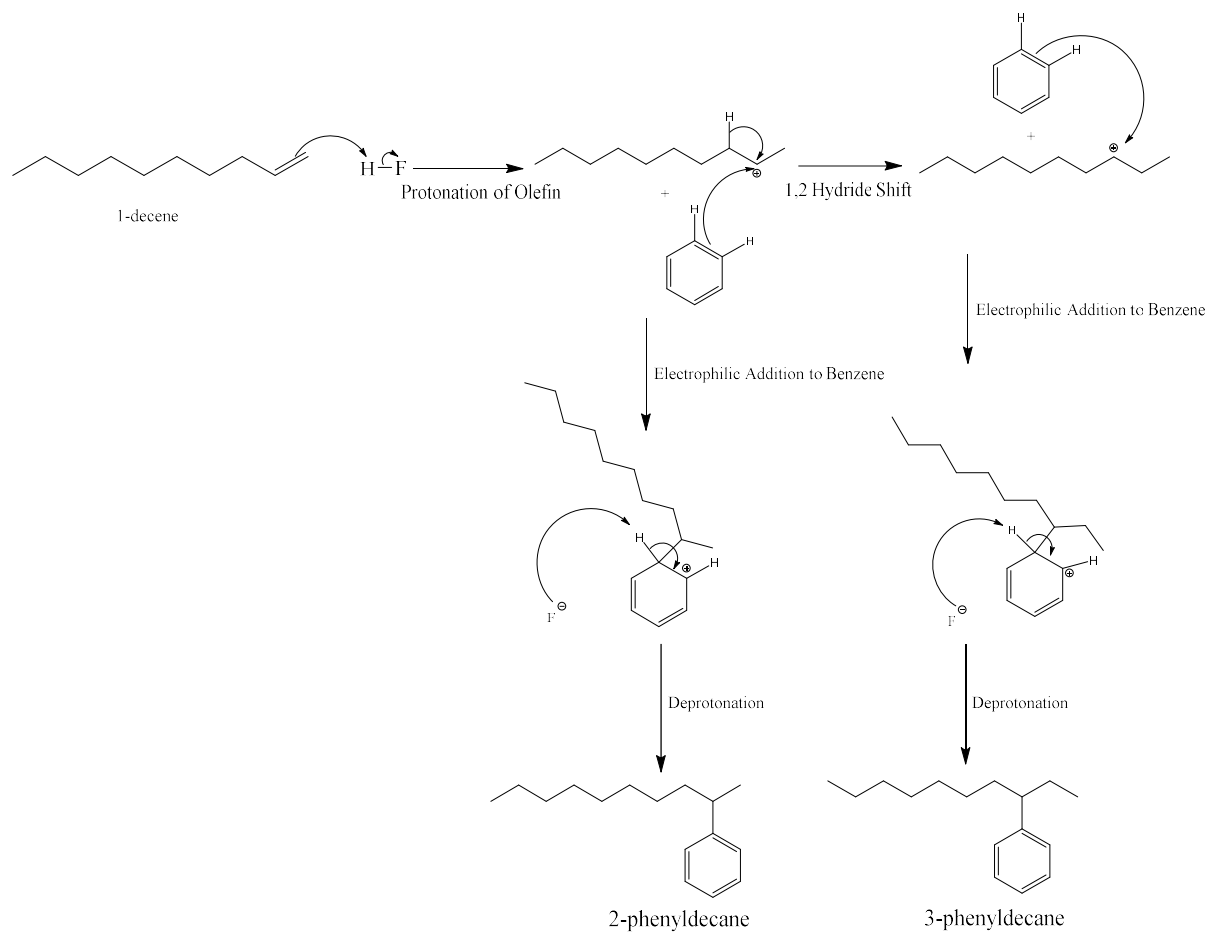


Figure 1. Friedel Crafts alkylation of benzene mechanism

Biodegradability and solubility of LAS greatly depends on the structure of the alkyl chain and the position of the phenyl group. LAS skeletal isomers have the general formula  $\text{C}_6\text{H}_4\text{C}_n\text{H}_{2n+1}\text{SO}_3\text{Na}$  where  $n$  is 8-16 typically<sup>4</sup>. Figure 2 displays the general structure of LAS. There are several possible skeletal isomers of LAS according to the position of attachment between the phenyl group and the carbon of the alkyl chain. Out of the isomers of LAS, the sodium 2-phenylalkane sulfonates (Na-2-LAS) has shown the highest biodegradability and the lowest solubility<sup>5</sup>. Thus, the ideal LAS surfactant needs a compromise between the biodegradability and solubility to encourage environmental health and to remain effective.

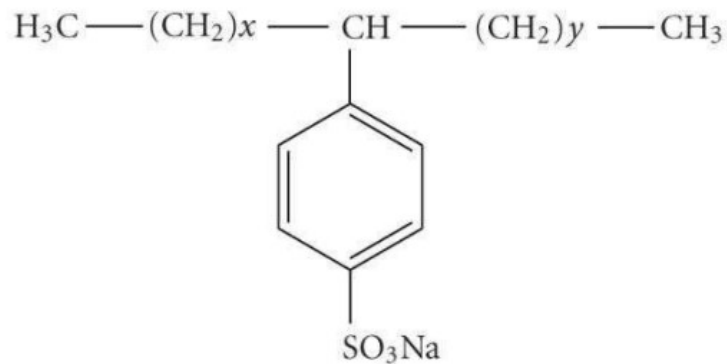


Figure 2. General structure of LAS ( $\text{C}_6\text{H}_4\text{C}_n\text{H}_{2n+1}\text{SO}_3\text{Na}$ )

The manufacture of linear alkyl benzenes (precursors to LAS) is a vast industry where around 70% of the 29.3 million tons of benzene demand was utilized in the alkylation of aromatics in the year 1999<sup>4</sup>. The industrial production of LABs has proceeded through several methods in the past. First, long-chain alkanes (paraffins) of 10-14 carbons long are isolated from oil gas fractions through a multitude of techniques and adsorptive separations. This step of the process may be carried out in a variety of phases. For instance, the Molex technique uses liquid phase hydrocarbon adsorbent along with a moving bed technology while Exxon Ensorb is a vapor phase process. Both techniques recover the paraffins at very high purity (around 98%)<sup>6</sup>.

Once the paraffins are isolated, several different routes could be taken to modify them in preparation for the alkylation benzene. One common method in the past was to chlorinate the paraffins and form mono-chlorinated paraffins. During the industrial process, the mono-chlorinated paraffins were used with aluminum chloride to alkylate benzene. This method for the alkylation of benzene producing LABs was originally developed for commercial use by ARCO Technology, Inc.<sup>6</sup> Another method in the alkylation of benzene is a dehydrochlorination of the mono-chlorinated paraffins to create alkenes (olefins)<sup>7</sup>. The subsequent olefins can then be utilized to alkylate benzene catalyzed by a Lewis acid. Several companies such as Chevron

Corporation harness ethylene oligomerization to produce these long-chain olefins with the use of hydrofluoric acid as the acid catalyst in the alkylation process<sup>5</sup>.

Until the late 1960s, the alkylation method utilizing aluminum chloride as the catalyst was the predominant pathway of producing LABs until the method involving dehydrochlorination and the use of hydrofluoric acid was introduced and popularized. After the late 1960s, the route utilizing hydrofluoric acid and olefins was the most popular technique of catalysis in the LAB synthesis due to the high quality of LABs produced and the low cost of the kerosene feedstock commonly used in the dehydrogenation of paraffins precursor step to create olefins<sup>8</sup>.

Unfortunately, the use of homogeneous acid catalysts like hydrofluoric acid has raised concerns. Primarily, the use of such catalysts results in large amounts of toxic waste which harms the environment and corrodes the expensive industrial equipment utilized in the catalysis. In general, the use of homogenous acid catalysts in the alkylation of benzene displays handling, containment, separation, and regeneration issues<sup>9</sup>.

Solid catalysts have since been proposed as a possible solution to the multitude of concerns with homogenous acid catalysts such as hydrofluoric acid. During the 1990s, the first commercialized process, which utilized solid catalysts was the Detal<sup>TM</sup> process. This process was created by Honeywell Universal Oil Products (UOP) and is the only modern technology that uses solid catalysts in the process of benzene alkylation. Another commercial process is under review and development in India at the moment, which utilizes a zeolite-based catalyst<sup>6</sup>.

The UOP Detal<sup>TM</sup> process has two steps. First, normal paraffins must be produced. During this step of the process, the heavy components and light ends of kerosene feedstock are stripped by prefractionation in order to produce n-paraffins. In preparation for the Molex, the kerosene is hydrotreated to remove sulfur, nitrogen, olefins, and other compounds which may adversely



affect the Molex adsorbent in the following step. The Molex process finally separates the normal paraffins from the cyclic or branched components. The second section of the process results in the production of LABs via the Detal™ process after several precursor steps designed to form mono-olefins from the normal paraffins. The Detal™ process operates in a fixed bed reactor with a solid catalyst. The flow scheme of the process can be seen below in Figure 3<sup>10</sup>.

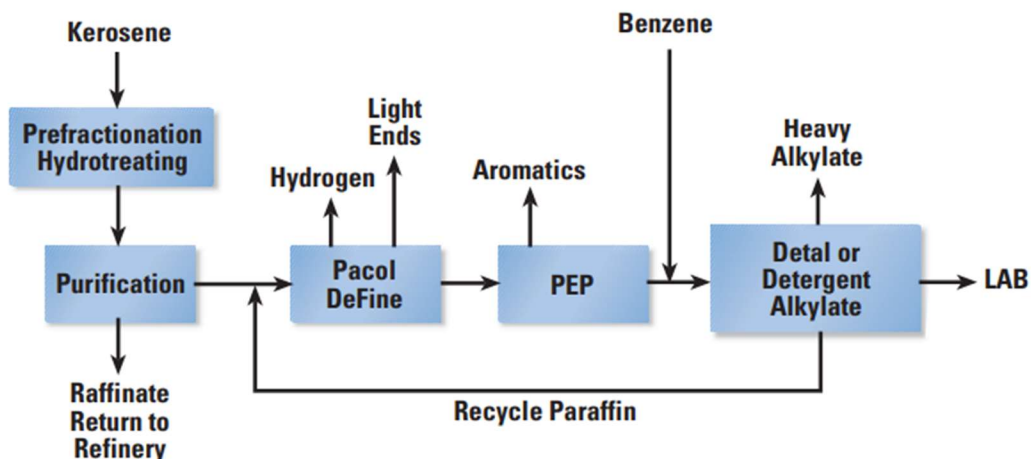


Figure 3. Detal™ process flow scheme<sup>10</sup>

In summary, homogeneous Brønsted and Lewis acids such as  $\text{H}_2\text{F}_2$ ,  $\text{HCl}$ ,  $\text{ZnCl}_2$ , and  $\text{AlCl}_3$  have been utilized widely the past in many organic reactions requiring an acid catalyst. Unfortunately, these homogenous acid catalysts create multiple issues in handling, instrument corrosion, environmental waste, and regeneration in industrial processes. Thus, interest has been shown in replacing the traditional homogeneous acid catalysts with catalysts that are more friendly, such as heterogeneous acid catalysts<sup>9</sup>.

## 1.2 Heterogenous Catalysts

Heterogenous catalysts' use in organic reactions has gained recognition due to their multiple redeeming factors and have previously been used in many protection and deprotection reactions<sup>11</sup>. The heterogenous catalysts offer mild reaction conditions, straightforward product

isolation, regeneration (and subsequent reuse) of the catalyst, and less toxic waste produced from the reaction<sup>12,13</sup>.

Heterogenous catalysts such as solid acid catalysts and supported acid catalyst complexes have successfully been utilized in organic reactions such as several types of alkylation and disproportionation of aromatic compounds with only minor issues. Liquid acids such as those based on metal fluorides and chlorides, on the other hand, face several problems by catalyzing unwanted side reactions. These reactions initiated by liquid acids results in isomerization, polymerization, and alkene degradation. The liquid catalyst also proves difficult to recover from the mixture and corrodes the vessels where the reaction takes place<sup>14</sup>. However, liquid acids are active in the organic reactions below 100 °C while solid supported and aluminosilicate acid catalysts require higher pressures and temperatures up to 200 °C<sup>15</sup>.

Activated clays and aluminosilicates have been used in the alkylation of benzene since the 1940s due to their higher activity and thermal stability than ion exchange resins at certain temperatures. The clay and the synthetic aluminosilicate displayed good catalytic characteristics between 120 and 140 °C in the alkylation of benzene with C<sub>9</sub>-C<sub>12</sub> olefins<sup>15</sup>. Solid supported transition metal halides such as Tantalum (V) and Niobium (V) were also successfully used to catalyze the alkylation of benzene with C<sub>8</sub>-C<sub>10</sub> olefins<sup>16</sup>. On top of that, it has been reported that a silicotungstic acid (HSiW) was used to catalyze the alkylation of benzene with C<sub>11</sub>-C<sub>14</sub> olefins while the catalyst was supported on aluminosilicate or silica gel. The results of the catalysis with the supported HSiW showed that the activity of the acid catalyst depended on both the surface area and the molar ratio between the aluminum oxide and the silicon dioxide (Al<sub>2</sub>O<sub>3</sub>:SiO<sub>2</sub>) in the support. Despite the lower activation energy of 12-13 kJ/mol, the alkylation catalyzed by the

HSiW proceeded at a slow rate suffering from slow internal diffusion of reactants through the catalyst<sup>17</sup>.

In a similar study, aluminum-magnesium silicate with clay or zeolite structure was impregnated with various acid halides and used as an acid catalyst in the alkylation of benzene. The solid catalyst showed a conversion rate of long-chain olefins to alkylbenzenes of 95% with 85% selectivity. The same catalyzed reaction was studied when the clay form of the catalyst included cerium nitrate and was air-streamed at 600 °C. The alkylation of benzene with this form of the catalyst was carried out under pressure of 3.5 MPa at 150 °C. These catalyzed reactions yielded 99% conversion of the olefins into alkylbenzene with a 95% selectivity<sup>17</sup>.

Zeolites are solid alternative catalysts that have been evaluated in the alkylation of benzene in the past. Zeolites are microporous aluminosilicate minerals known as molecular sieves which are used in catalysis. Zeolite Y, modified by rare earth elements, was utilized in the alkylation of benzene with  $\alpha$ -olefins C<sub>10</sub>-C<sub>18</sub> long. An 85-90% conversion of the olefins was recorded in this instance when a molar ratio of 100:1 benzene to olefin was used along with a space velocity of 0.25 per hour<sup>18</sup>. Large pore zeolite Y along with zeolite Beta were further tested in 2001 which showed high stability but low selectivity in the reaction of benzene alkylation<sup>4</sup>.

Another type of zeolite, a lanthanide promoted zeolite, was used to catalyze the alkylation of benzene at 180 °C. The reaction resulted in a 94% yield of undodecylbenzene. When a high silica pentasil zeolite with an increased molar ratio of silica to alumina was used in the alkylation of benzene by dodecene at 220 °C, the conversion rate of the reaction jumped from 30 to 69%<sup>18</sup>.

Overall, various zeolites offer substantial benefits, such as high relative acidity and activity in the alkylation of benzene reaction. However, application of these solid catalysts is limited by some major drawbacks. For instance, Mobil Oil Corporation studied the zeolites ZSM-5 and

ZSM-12 in 1981. ZSM-5 showed low selectivity which ZSM-12 improved upon, but ZSM-12 displayed low yield of alkylbenzenes in the reaction<sup>19</sup>. A similar circumstance took place with the zeolites ERB-1 and L where both showed high activity and selectivity in the reaction but were unstable<sup>4</sup>. Zeolites were shown to be irreversibly deactivated in the process which complicates the regeneration and reuse of the catalysts failing to solve some of the problems seen in homogenous catalysts. Thus, the search for more efficient solid catalysts has been promoted.

### 1.3 Heteropolyacids

Heteropolyacids (HPAs) is a class of superacids that have recently been recognized due to their excellent catalytic potential. HPAs are classified as superacids, which are acidic compounds with a  $pK_a$  of at least 100% greater than sulfuric acid. Not only are HPAs highly acidic, but they are also known for their redox properties which can be altered by changing the composition of the heteropolyanion. Previously, both homogenous and heterogenous HPAs have been studied which has shown the multitude of reactions they may be applied in. HPAs have been shown to catalyze reactions such as alkylation, dehydration, cyclization, and even oxidation of amines leading to applications in many fields like the food and pharmaceutical industries<sup>20</sup>. The Wells-Dawson and Preyssler structured HPAs have been evaluated as well, but the most used HPAs possess the Keggin anion structure due to its high stability and catalytic activity<sup>21</sup>.

HPAs with the Keggin anion structure are polynuclear complexes that consist of polyatoms (M) such as tungsten, molybdenum, or vanadium, and consist of a central heteroatom such as phosphorous, germanium, or silicon<sup>22</sup>. The central portion of the Keggin anion is made of a tetrahedral hetero atom oxide as a  $XO_4$  which is surrounded by twelve octahedral polyatom oxides  $MO_6$ . Thus, the Keggin anion as seen in Figure 4<sup>23</sup> has a general molecular formula of  $[XM_{12}O_{40}]^{3-}$ <sup>(24)</sup>. The other two types of HPAs, the Wells-Dawson and the Preyssler have varying

combinations of these atoms as compared to the Keggin anion structure. For the Wells-Dawson structure, the heteropoly anion has a formula of  $[X_2^{n+}M_{18}O_{64}]^{n-}$  where the hetero atom (X) is a central sulfur, arsenic, or phosphorus atom surrounded by 18 polyatoms (M) such as tungsten or molybdenum paired with oxygen in an octahedral block. The structure is called an alpha isomer which consists of two central atoms that each are a “half unit” of the complex which are surrounded by the octahedral blocks<sup>25</sup>. Developed from the Keggin anion, the Preyssler structure is a cyclic complex consisting of five  $PW_{12}O_{22}$  subunits where two groups of 3 corner  $WO_6$  octahedra<sup>26</sup>.

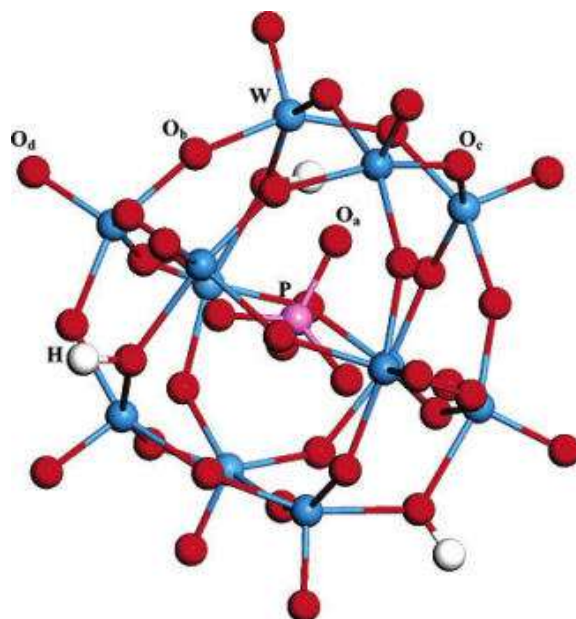


Figure 4. Keggin structure  $H_nXM_{12}O_{40}$  consisting of phosphorous (pink) as X, tungsten (blue) as M, oxygen (red) and hydrogen (white).<sup>23</sup>

As compared to zeolites, such as zeolite Y, HPAs offer several improvements as evidenced in an evaluation of catalytic properties of phosphotungstic acid  $H_3PW_{12}O_{40}$  (PTA), and zeolite Y. PTA demonstrated increased stability, catalytic activity, and selectivity when compared to

zeolites in the same reaction of benzene alkylation with 1-dodecene. The reaction was carried out at 80 °C and a conversion of 90% of the olefin with a near 100% selectivity for LABs<sup>27</sup>.

Despite the results of the comparison to zeolites, the use of pure HPAs also still poses many complications. Like the homogenous catalysts many are working to replace, the pure HPA is difficult to separate from the product mixture at the end of the reaction, which hinders its recyclability and increases waste production. Furthermore, HPAs are highly soluble in polar solvents and possess a low surface area which affects the catalytic efficiency.

#### **1.4 Supported Heteropolyacids**

Impregnating acids on solid supports is a technique that has gained attention due to the multiple improvements it provides. HPAs demonstrate high catalytic activity and stability but suffer from a low surface area. However, the development of solid supported HPAs opens new routes for the use of efficient catalysts. Silicate supported acids, such as perchloric acid, have been utilized more and more in the catalysis of organic reactions, which demonstrate the advantages of supported super acids. As a result of the larger surface area provided by the silica support, the supported acids have shown an increased catalytic efficiency. In addition, the silica supported acids showed a higher thermal stability, selectivity, and recyclability as well as reduced toxicity to individuals during handling<sup>28</sup>. Polymer based supports have also been used in catalysis but had limitations when compared to the silica supports.

Preparation of the mesoporous silica supported catalysts may be carried out through several methods such as ion exchange, impregnation, covalent grafting, electrostatic forces, and the sol-gel technique<sup>29</sup>. For the immobilization of HPAs, however, two main processes have been utilized for the immobilization on silica support: impregnation and the sol-gel technique<sup>30</sup>.

Impregnation on the support, which involves a much weaker interaction, has been the most widely used method prior to this research.

During impregnation of HPAs on a pre-assembled silica support, the structure is altered which causes less homogeneity. Impregnation also leaves the HPAs vulnerable to leaching since the catalyst is not embedded in the support. Rather, the HPA is loaded onto the surface of the silica which also decreases the stability and activity of the catalyst<sup>31</sup>.

The silica supported HPAs present numerous advantages as evidenced by their use previously in organic reactions. The impregnated PTA-SiO<sub>2</sub> was used in various reactions such as the 3,4-dihydropyrimidones from aldehyde, urea, and keto-ester in acetonitrile<sup>32</sup>. In comparison to other classical methods like the Biginelli method, catalysis with supported HPAs is more convenient to work with and show high yields, functional group tolerance, and mild conditions in the reactions which they catalyze. For instance, the gas-phase alkylation of phenol with tert-butanol catalyzed by phosphotungstic (tungstophosphoric) acid (PTA), which is an HPA, showed a high selectivity for the desired para-tert-butylphenol product<sup>33</sup>. Furthermore, silicated HPA supported on an MCM-41 support was studied in the catalysis of the liquid-phase alkylation of toluene with 1-octene. The HPAs studied were PTA, tungstosilicic acid (HSiW), and molybdophosphoric acid (HPMo) supported on the MCM-41, and bulk HPA. Compared to just the bulk HPA, the MCM-41 supported HPAs showed higher activity with a near 100% conversion and high selectivity of only monoalkylated products. The study demonstrated the importance of the surface area of the catalyst as the higher surface area MCM-41 supported HPAs outperformed the bulk HPA in efficiency of catalysis. The supported catalysts were also found to be reusable<sup>34</sup>.

The sol-gel method, also applicable in preparation of supported HPAs, involves a co-condensation synthesis where a sol is formed, cross-linked, and a gel results. The silica precursors and HPA are condensed and hydrolyzed in a polar solvent as seen in Figure 5. After polymerization, a highly cross-linked 3-D network is created. The process is sped up greatly upon addition of an acid or base in the system, but an acid is preferred in the case of HPAs as they are unstable in the presence of a base<sup>31</sup>.

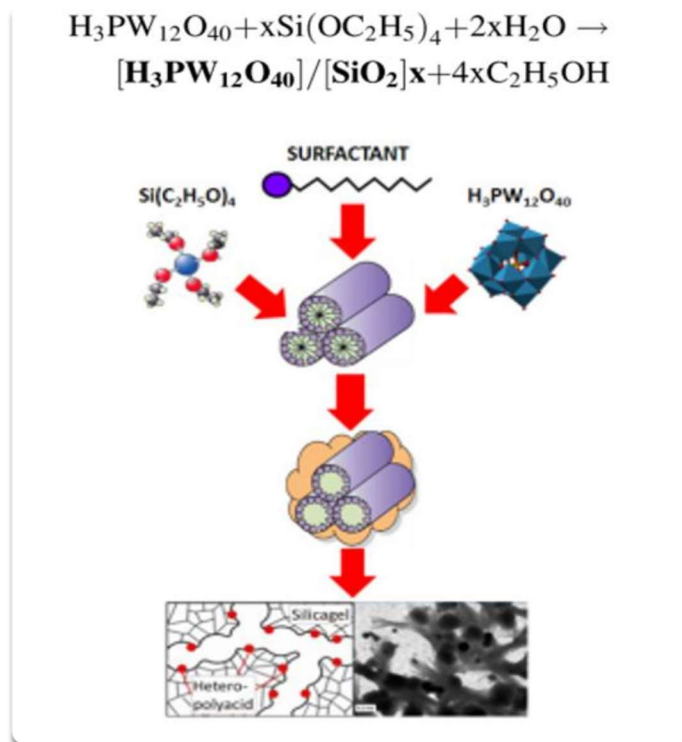


Figure 5. Sol-gel synthesis of PTA-SiO<sub>2</sub> catalyst

HPAs are integrated into the silica via co-condensation of HPA clusters with silicon oxide precursor. This creates strong Si-O-W covalent bonds which embed the HPA in the silica support. Surfactants are also introduced to create a highly mesoporous catalyst which is vital for creating a large surface area where active sites are evenly distributed. The highly mesoporous catalyst has increased stability and greater performance in the catalysis<sup>35</sup>. The sol-gel



technique is preferred over impregnation due to the decreased leaching as a result of covalent bonding between the HPA and silica.

Previously, this method of catalyst immobilization was completed and utilized successfully in the liquid phase alkylation of benzene. In comparison to pure liquid phase PTA, the covalently embedded PTA-SiO<sub>2</sub> showed a much higher yield of the phenyl alkane target products. In addition, it was noted that the conversion percent of various alkenes in the process depended on chain length with 1-octene showing the highest conversion compared to 1-decene and 1-octadecene<sup>36</sup>.

Similarly, the covalently embedded PTA was used in the catalysis alkylating 1,3,5-trimethylbenzene with 1-decene. The PTA-SiO<sub>2</sub> showed high catalytic activity in the reaction exceeding the activity of the HY zeolite. The results of this work also demonstrated that the covalently bound PTA in the support successfully prevented leaching. The prevention of leeching shows promise for the recyclability of the catalyst in the process<sup>37</sup>.

## **1.5 Research Objectives**

During previous work in this project, the liquid phase alkylation of benzene by olefins with the supported phosphotungstic acid was evaluated utilizing a powder form of the PTA-SiO<sub>2</sub> catalyst in a pressurized batch reactor. The objectives of this research are to synthesize and evaluate the catalytic performance of a granulated form of the silica supported PTA in the gas phase alkylation of benzene with olefins and generation of alkene isomers in a fixed bed flow reactor.

## II. Experimental

### 2.1 Reagents and Materials

The chemicals utilized during the work on this project are listed below in Table 1.

Table 1. Chemicals utilized

Reagent	Molecular Formula	Supplier	Application
Phosphotungstic acid hydrate (PTA)	$H_3[PW_{12}O_{40}] \cdot xH_2O$	Acros Organics (Morris Planes, NJ)	Catalyst precursor
1-Decene	$CH_3(CH_2)_7CH=CH_2$	Acros Organics (Morris Planes, NJ)	Reactant
1-Octene	$CH_3(CH_2)_5CH=CH_2$	Acros Organics (Morris Planes, NJ)	Reactant
1-Octadecene	$CH_3(CH_2)_{15}CH=CH_2$	Alfa Aesar (Tewksbury, MA)	Reactant
Benzene	$C_6H_6$	EMD Millipore Corp (Darmstadt, Germany)	Reactant
Hexane	$C_6H_{14}$	J.T. Baker (Phillipsburg, NJ)	Solvent
Hydrochloric acid	HCl (35%)	Fisher Chemical (Pittsburgh, PA)	Catalyst
Pluronic P123	$HO(CH_2CH_2O)_{20}(CH_2CH(CH_3)O)_{70}CH_2CH_2O)_{20}H$	Sigma-Aldrich (St. Louis, MO)	Surfactant
Tetraethyl orthosilicate (TEOS)	$Si(OC_2H_5)_4$	Acros Organics (Morris Planes, NJ)	Catalyst precursor
Hydrofluoric acid	$H_2F_2$ (50%)	VWR BDH Chemicals (Radnor, PA)	Reactant
Ammonium hydroxide	$NH_4OH$ (25%)	Acros Organics (Morris Planes, NJ)	Reactant
$\gamma$ -Alumina	$Al_2O_3$	Strem Chemicals Inc. (Newburyport, MA)	Binding agent

## 2.2 Catalyst Preparation

### *Sol-Gel Synthesis*

As described, the sol-gel synthesis method was used to prepare the supported PTA-SiO<sub>2</sub> catalyst. Two solutions were made, one contained 50 g of the Pluronic P123 surfactant dissolved in 150 mL of ethanol. A PTA and TEOS solutions was also prepared by dissolving 72 g of TEOS and 18 g of PTA in 50 mL of ethanol. The PTA and TEOS solution along with a 150 mL 20% HCl solutions were dropwise added into the surfactant solution while being stirred. A gel was formed after refluxing the solution for 24 h, which was subsequently first washed with deionized water to remove the leftover acid and washed again with acetone. After drying overnight, the washed gel product was calcined at 500 °C for 4 h to remove the surfactant<sup>38</sup>.

### *Catalyst Pre-Treatment*

Prior to use in alkylation, the supported catalyst required granulation for use in a flow reactor. The hard catalyst powder needed to be combined with a softer, inert powder as a binding agent. Aluminum oxide was utilized as the binding agent and combined with the PTA/SiO<sub>2</sub> in a 1:1 mass ratio. The mixture was packed into tablets in a Carver 13 mm pellet die placed in a bench top manual pellet press model 4350.L (Carver, Inc., Wabash, IN) (Figure 6) under a pressure of 10,000 psi. The powder was pressed between two cylinders in a sleeve under a press for 10 minutes. The tablets were then granulated to a diameter of 0.5 – 1.0 mm in diameter in a sieve. Afterwards, the granules were calcined at 400 °C for two hours to remove any moisture.

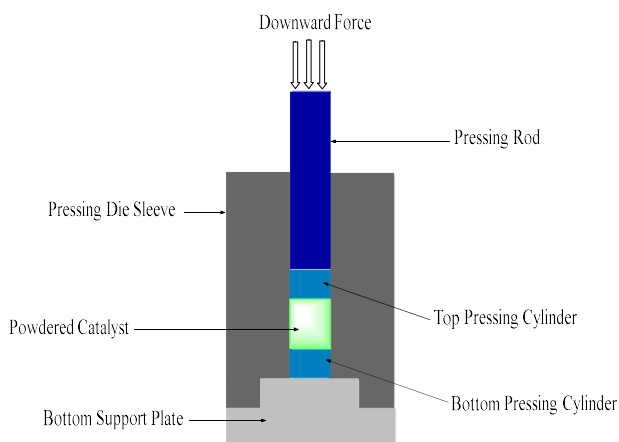


Figure 6. Carver 13 mm pellet die used to form tablets.

## 2.3 Instrumental Characterization

### *Elemental Analysis*

Flame atomic absorption spectroscopy (AAS) with a tungsten lamp was utilized to measure the contents of tungsten in the samples. The goal of this characterization was to quantify how much PTA had been leached from the silica support. A Shimadzu AA-6300 atomic absorption spectrometer (Kioto, Japan) was utilized to analyze the samples. These samples were first dissolved in hydrofluoric acid and then neutralized to a pH of 7 with 25% aqueous ammonia solution. This process resulted in the formation of a tungstate ion  $\text{WO}_4^{2-}$  as well as soluble ammonium silicate. The AAS was used to analyze the concentration of tungstate ion in each solution.

The elemental analysis of organic carbon was provided by the Robertson Microlit Laboratories (Ledgewood, New Jersey).

### *Fourier-Transform Infrared Spectroscopy*

KBr pellets were made and used to record FT-IR spectra of the materials on a Mattson Genesis II spectrometer (Madison, WI). The solid material was grinded with a mortar and pestle

along with the KBr into a fine powder. The powder was then pressed into a tablet and placed in the instrument for recording.

#### *Scanning Electron Microscopy*

The Zeiss DSM 940 scanning electron microscope (Oberkochen, Germany) was utilized to generate SEM images of the catalyst at 20 kV. Prior to SEM imaging, the catalyst was coated in gold.

#### *BET Surface Area*

The porous characteristics of the catalyst were measured using a Quantachrome Nova 2200e porosimeter with NovaWin v.11.02 software (Boynton Beach, FL). Before the measurement, each sample was degassed under a vacuum for two hours at 400 °C. Nitrogen gas was used in the determination of the surface area at -196 °C.

#### *Particle Size Distribution*

Particle sizes were measured by dynamic light scattering (DLC) using a Zetasizer Nano ZS90 (Malvern, UK) instrument. Prior to each measurement, the samples were placed in de-ionized water and dispersed under sonication for 5 min.

#### *Analysis of Reaction Mixtures*

A Shimadzu GCMS-QP20210 Plus gas chromatograph (Kioto, Japan) was utilized to separate the alkene isomers and to quantify the peak areas. Each sample was diluted by hexane and then placed in the GC-MS loader. Injections of 1  $\mu$ L were made into the Rtx-5MS capillary column where helium was used as a carrier gas with a flow rate of 21.9 mL/min. The alkene mixtures were analyzed with an oven temperature of 40 °C and injector temperature of 280 °C.

A Thermo Scientific Trace 1300 Gas Chromatograph with flame ionization detector (FID) was used in the analysis of the product mixture resulting from the catalytic alkylation of benzene by 1-decene. The GC-FID instrument contained a 7 m by 0.32 mm ID Thermo TR5 column with a 0.25 mm film thickness used in the analysis of the product mixtures. The samples were diluted by hexane similarly to the GC-MS analysis and 1  $\mu$ L injections were made with a 280 °C injector temperature and a 50 °C oven temperature. The vaporized product mixture was flowed through the column with a 16.2-minute run time and gas flow rate of 5 mL/min. Helium was utilized in the column as a carrier gas with a flow rate of 40 mL/min.

## 2.4 Catalytic Properties

### *Isomerization of Alkenes*

Prior to the catalytic reaction, the granulated PTA-SiO<sub>2</sub>/Al<sub>2</sub>O<sub>3</sub> was calcined at 400 °C for 2 h to remove moisture. Two grams of the catalyst were then combined with equal amount of granulated glass. The mixture was loaded into a fixed bed in the flow reactor and then covered with a thin layer of more granulated glass. Before the reaction, nitrogen was cycled through the reaction column to remove any oxygen present preventing unwanted oxidation. An alkene (20 mL) with identities of either 1-decene, 1-octene, or 1-octadecene in a syringe was injected into the 200 °C heated reactor for 1 h creating a flow rate of 10 mL/(g<sup>-1</sup>h<sup>-1</sup>). The vaporized alkene recondensed into a collection flask once it flowed through a water-cooled condenser at the bottom of the apparatus (Figure 7).

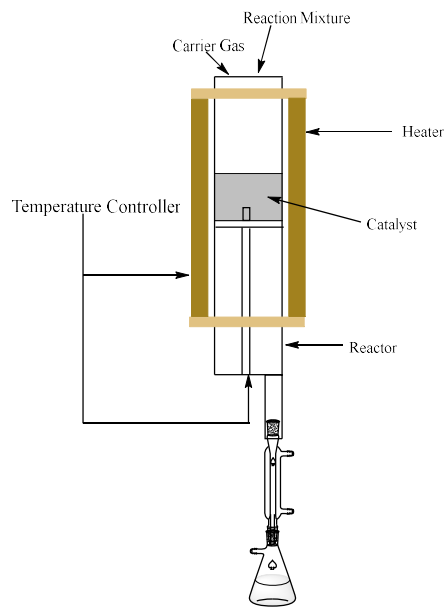


Figure 7. Fixed bed flow reactor used in the isomerization of alkenes and alkylation of benzene reactions.

### *Alkylation of Benzene*

The catalytic alkylation of benzene reaction was carried out similarly to the isomerization reactions in a fixed bed flow reactor (Figure 7). During catalyst pre-treatment, 1-4 g (depending on target flow rate) of the PTA-SiO<sub>2</sub>/Al<sub>2</sub>O<sub>3</sub> were calcined at 400 °C for 2 h, combined with granulated glass, and placed in the column in the same fashion as the isomerization experiments. The column was also flushed with nitrogen to remove any oxygen present. The reaction was carried out with 20 mL of 2-8:1 molar ratio benzene to 1-decene. This mixture was injected into the column which was heated to 200-250 °C. The mixture was vaporized, flowed over the bed of catalyst, condensed in the water-condenser, and collected in a flask (Figure 7).

### III. Results and Discussion

#### 3.1 Physical Characteristics and Chemical Composition

##### *Immobilized PTA-SiO<sub>2</sub>*

Once sol-gel synthesis was performed to immobilize the PTA in a silica matrix, a hard, light yellow powder resulted. This powder's chemical structure consisted of the silica gel and PTA covalently embedded into the silica support with an oxygen bridges between Si and W atoms. The powder was very hard leading to an incompressibility of the pure PTA-SiO<sub>2</sub>.

The catalyst was characterized via FT-IR to identify structural characteristics of the catalyst as seen in Figure 8. According to literature, the silica is characterized by IR peaks at 805, 1088, and 1654 cm<sup>-1</sup>. As seen in the IR spectrum obtained from the pure PTA-SiO<sub>2</sub> in Figure 8 (1), the sample displayed an intense broad peak at 1088 cm<sup>-1</sup>, a peak at 808 cm<sup>-1</sup>, and another distinct peak at 1654 cm<sup>-1</sup>. These three characteristic peaks confirm the presence of the silica matrix in the powder sample. Furthermore, literature states that O-W-O stretch of the phosphotungstic acid is visible as a broad peak at 963 cm<sup>-1</sup>. Figure 8 (1) also displays a clear peak occurring at 962 cm<sup>-1</sup> indicating that the PTA was embedded in the silica matrix successfully<sup>39</sup>.

Atomic absorption analysis (AAS) was utilized to determine PTA contents in the catalyst. Based on the absorbance signal, the concentration of tungsten corresponded to a PTA content of 0.051 mmol/g as shown in Table 2.

The porosity of the PTA-SiO<sub>2</sub> powder catalyst was also surveyed with BET surface area measurement. This parameter is vital for catalytic activity in the reaction. The average surface area of PTA-SiO<sub>2</sub> was measured to be 476.9 cm<sup>3</sup>/g (Table 2).



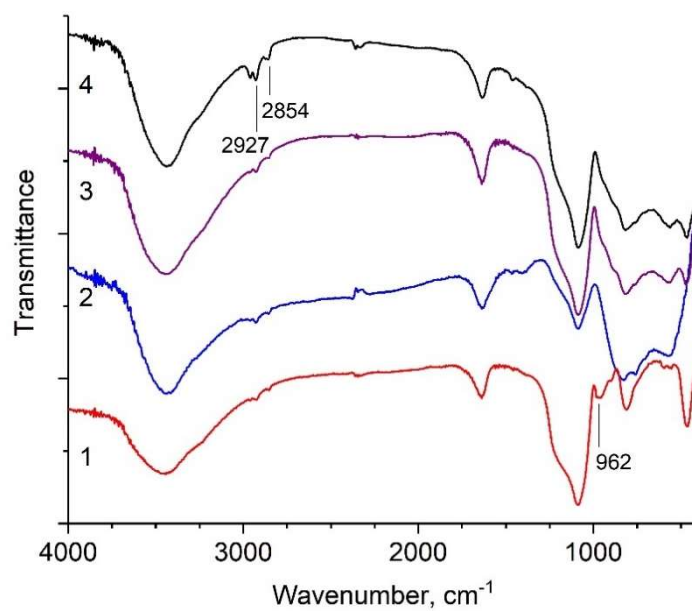


Figure 8. FT-IR of the catalysts: PTA-SiO<sub>2</sub> (1),  $\gamma$ -Al<sub>2</sub>O<sub>3</sub> (2), PTA-SiO<sub>2</sub>/Al<sub>2</sub>O<sub>3</sub> (3), and post-reaction PTA-SiO<sub>2</sub>/Al<sub>2</sub>O<sub>3</sub> (4).

Table 2. Catalyst characteristics

Sample	Contents of PTA, mmol/g	BET surface area, cm <sup>3</sup> /g	Mean particle size, nm	PDI	Carbon contents, wt.%
PTA-SiO <sub>2</sub>	0.051	476.9	676	0.845	-
$\gamma$ -Al <sub>2</sub> O <sub>3</sub>	-	61.8	819	0.949	-
PTA-SiO <sub>2</sub> /Al <sub>2</sub> O <sub>3</sub> (fresh)	0.027	168.3	856	0.935	-
PTA-SiO <sub>2</sub> /Al <sub>2</sub> O <sub>3</sub> (spent)	0.026	176.4	787	0.843	13.04

SEM and DLS were utilized to determine the particle size of the PTA-SiO<sub>2</sub> and the polydispersity index (PDI). A SEM image of PTA-SiO<sub>2</sub> (Figure 9) showed large agglomerates of spherical particles of up to 5  $\mu$ m and many smaller particles of silica with diameters between 300 and 600 nm<sup>38</sup>. The average particle diameter was measured by DLC to be 676 nm with a PDI of

0.845 (Table 2). The PDI indicates the dispersity of samples where a value closer to 1 indicates a disperse mixture while a value of zero shows a more homogenous powder. In the case of the PTA-SiO<sub>2</sub>, the PDI was 0.845 indicating a fairly disperse powder.

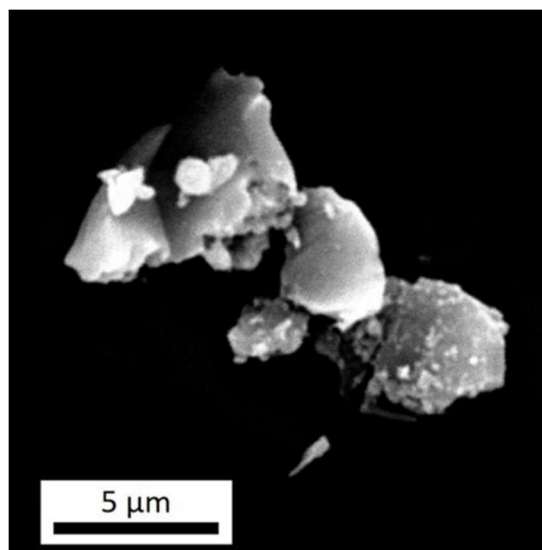


Figure 9. SEM image of PTA-SiO<sub>2</sub><sup>38</sup>

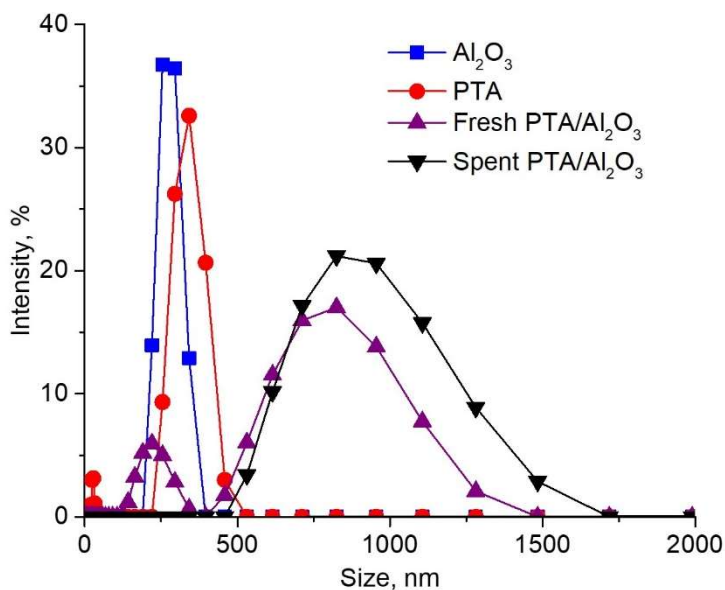


Figure 10. Particle size distribution (nm) for PTA-SiO<sub>2</sub>,  $\gamma$ -Al<sub>2</sub>O<sub>3</sub>, fresh PTA-SiO<sub>2</sub>/Al<sub>2</sub>O<sub>3</sub>, and spent (post-reaction) PTA-SiO<sub>2</sub>/Al<sub>2</sub>O<sub>3</sub>.

### *$\gamma$ -Alumina Characteristics*

The white-powder  $\gamma$ -Al<sub>2</sub>O<sub>3</sub> was utilized as a binding agent for PTA-SiO<sub>2</sub> since the powder is much softer than the PTA-SiO<sub>2</sub> powder making it more easily compressed into tablets. Thus, the compound was analyzed via the same methods to account for any effects in the characterization of the catalyst. The literature FT-IR of  $\gamma$ -Al<sub>2</sub>O<sub>3</sub> has characteristic peaks at 1649, 997, 667, and 556 cm<sup>-1</sup><sup>40</sup>. As indicated by the experimental FT-IR of  $\gamma$ -Al<sub>2</sub>O<sub>3</sub> in Figure 8 (2), these characteristic peaks are present.

The BET surface area of  $\gamma$ -alumina is 61.8 cm<sup>3</sup>/g, giving it a much lower surface area than the PTA-SiO<sub>2</sub> catalyst itself (Table 2). The average particle size and PDI of  $\gamma$ -Al<sub>2</sub>O<sub>3</sub> were measured to be 819 nm in diameter and 0.949, respectively. The average particle size of  $\gamma$ -Al<sub>2</sub>O<sub>3</sub> is similar but slightly larger than the PTA-SiO<sub>2</sub> and the PDI shows the powder has broad dispersion of particle sizes.

### *Granulated PTA-SiO<sub>2</sub>/Al<sub>2</sub>O<sub>3</sub>*

The PTA-SiO<sub>2</sub> was combined with  $\gamma$ -Al<sub>2</sub>O<sub>3</sub> and granulated into 0.5-1 mm diameter pale yellow granules. This catalyst-alumina combination allowed for the PTA-SiO<sub>2</sub> to be compressed and used in the flow column during catalysis. The FT-IR spectrum of the PTA-SiO<sub>2</sub>/Al<sub>2</sub>O<sub>3</sub>, as shown in Figure 8 (3), displayed characteristic peaks of both compounds. Since the compounds share similar peaks such as the characteristic peak near 1000 cm<sup>-1</sup> and the one near 1650 cm<sup>-1</sup>, these peaks show little change compared to the other two spectra of each compound.

The average BET surface area of PTA-SiO<sub>2</sub>/Al<sub>2</sub>O<sub>3</sub> was measured as 168.3 cm<sup>3</sup>/g which decreased from the original surface area of PTA-SiO<sub>2</sub> due to being packed in granules with the much lower surface area  $\gamma$ -alumina particles. The average particle size of the PTA-SiO<sub>2</sub>/Al<sub>2</sub>O<sub>3</sub> was 856 nm in diameter which is also increased compared to that of the PTA-SiO<sub>2</sub>. The particle

size distribution (Figure 10) of PTA-SiO<sub>2</sub>/Al<sub>2</sub>O<sub>3</sub> shows a broader peak compared to the alumina and original PTA-SiO<sub>2</sub>. The polydispersity index, on the other hand, was measured to be 0.935 indicating a broad dispersion of particle sizes. (Table 2).

### 3.2 Catalytic Activity

#### *Isomerization of Alkenes*

After isomerization reactions were carried out in the fixed-bed flow reactor, the GC-MS analysis was completed to quantify the conversion rates of 1-alkenes to varying isomers. Figure 11 displays the GC-MS chromatograms of the isomerization products of 1-octene (1), 1-decene (2), and 1-octadecene (3). The red arrows indicate the starting 1-alkene while the other signals in the chromatogram belong to isomers such as 2, 3, or 4-alkene.

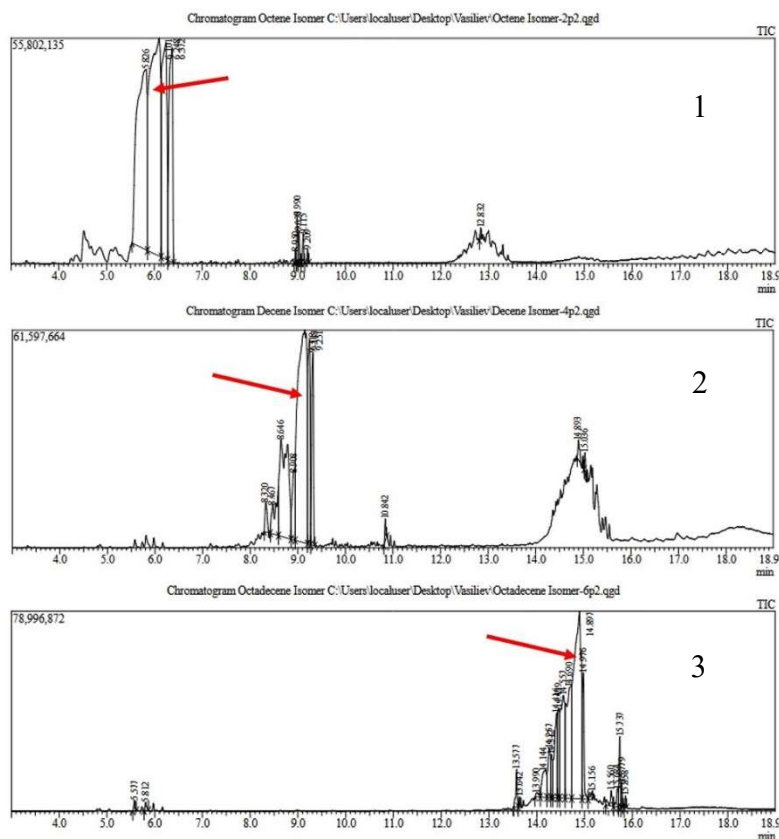


Figure 11. GC-MS chromatograms of 1-octene (1), 1-decene (2), and 1-octadecene (3).

High conversions of each alkene into their respective isomers were achieved during the reaction. The 1-octene showed 55% (1) conversion into the various isomers. The 1-decene had a 52% (2) conversion into isomers, the lowest conversion rate of the 1-alkenes. The 1-octadecene, on the other hand, had the highest conversion percent with 57% (3). These results are displayed in Figure 12. The 1-octadecene showed the highest conversion percent due to the nature of the reaction. The reaction was carried out at 200 °C which is a temperature well above the boiling points of both 1-octene and 1-decene. However, 1-octadecene has a boiling point of 315 °C. Therefore, the 1-octadecene underwent catalysis while in the liquid phase rather than the gas-phase like the other two alkene reactants. While the polymerized alkene created by side reactions usually deposits on the surface of the catalyst causing deactivation during gas-phase catalysis, the polymerized alkene is soluble in octadecene that was in the liquid phase. Thus, the polymer dissolved in the liquid 1-octadecene preventing the deactivation of the catalyst and allowing higher conversion into isomers.

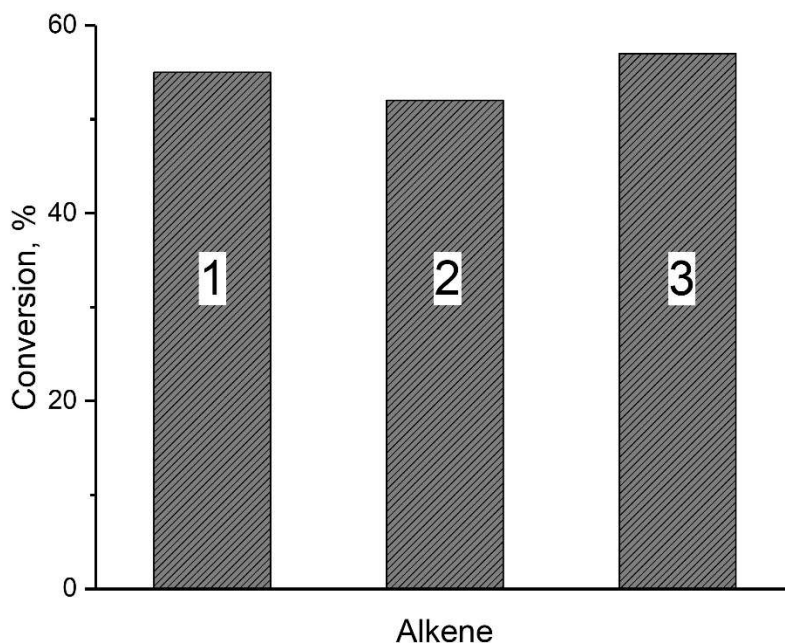


Figure 12. Conversions of 1-octene (1), 1-decene (2), and 1-octadecene (3) into isomers.

## Alkylation of Benzene by 1-Decene

The catalyzed alkylation of benzene with 1-decene was carried out in a fixed bed flow reactor. Figure 1 displays the general mechanism of the Friedel Crafts alkylation of benzene while Figure 13 shows the complexity of the isomerization of the reactants and products.

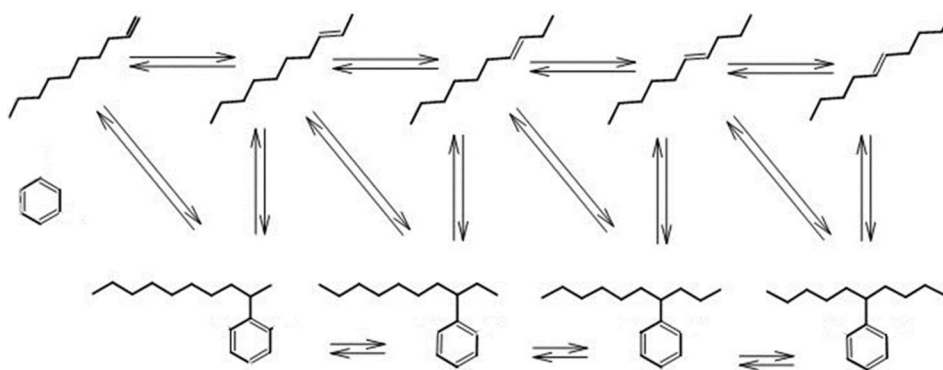


Figure 13. Alkylation of benzene with 1-decene and isomers formed

As seen in Figure 13, the protonated alkene undergoes a hydride shift causing the formation of multiple isomeric forms of the product phenyldecane. Depending on the isomer of decene that attaches to benzene, a benzene may be substituted on the carbon 2, 3, 4, or 5 position. Only trace amount of 1-substituted alkene was formed due to low stability of primary carbocations. GC-FID was used in the analysis of these alkylation mixtures with example chromatograms shown in Figures 14 and 15. Figure 14 displays the reactant mixture of benzene and 1-decene before the catalytic alkylation while Figure 15 shows the product mixture after catalysis.

As displayed in the reactant mixture chromatogram, two distinct peaks are visible, one at a retention time of 5.5 minutes and another at 5.7 minutes. The peak with more magnitude of a signal represents benzene while the other shorter peak represents the 1-decene. It is clear that before the reaction only one isomer of decene is present in the mixture, the starting material 1-decene.

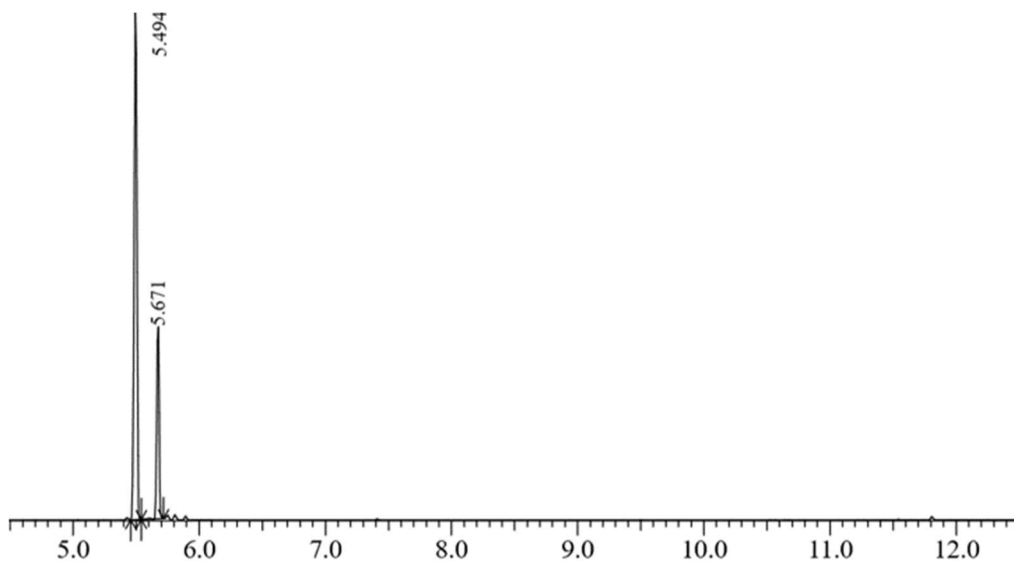


Figure 14. Reactant mixture of benzene (highest signal, 5.5 min.) and 1-decene (5.7 min.).

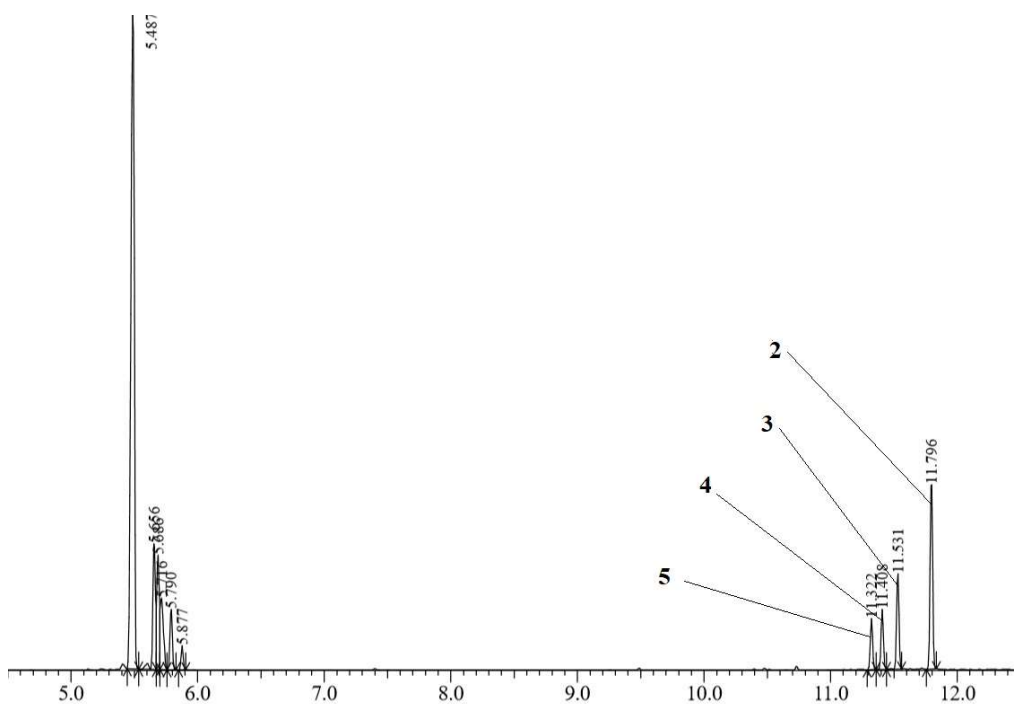


Figure 15. Product mixture of benzene (5.5 min.), decene isomers (5.6-6.0 min.), and phenyldecane isomers (11.2-12.0 min.).

After the catalytic reaction, several new signals may be seen in the chromatogram (Figure 15). The benzene signal at 5.5 min. remains relatively unchanged while the decene signal is split

into several different peaks representing isomers formed in the reaction. The products, isomeric phenyldecane, show signals near the end of the GC run time between 11.2 and 12.0 min. with 4 distinct isomer signals. From longest retention time to shortest retention time, the products were 2-phenyldecane, 3-phenyldecane, 4-phenyldecane, and 5-phenyldecane. Only a small amount of 1-phenyldecane was detected.

The conversion percent for each phenyldecane isomer was also investigated with a series of experiments performed at a flow rate of 10 mL/g (2 g catalyst), a molar ratio of benzene to 1-decene of 4:1, and a temperature of 250 °C. The results obtained from these experiments are displayed in Figure 16. The target product of the reaction, 2-phenyldecane was the predominant product among all isomers. The other isomers experienced lower yields with the order from highest yield to lowest being 3-phenyldecane, 4-phenyldecane, 5-phenyldecane, and 1-phenyldecane, respectively.

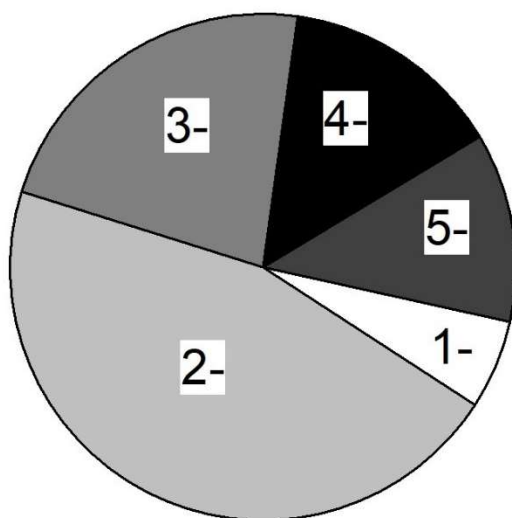


Figure 16. Phenyldecane isomers distribution

The catalytic activity of the PTA-SiO<sub>2</sub>/Al<sub>2</sub>O<sub>3</sub> in the alkylation of benzene with 1-decene was evaluated under varying reaction conditions. Several factors during the reaction were varied



including the flow rate of mixture in mL/g, the molar ratio of benzene to decene, and the temperature of the reaction. The flow rate was varied by utilizing different masses of the catalyst in the reaction where experiments proceeded with flow rates of 5, 10, and 20 mL/g. The molar ratio of benzene to 1-decene was varied as 8:1, 4:1, and 2:1. Figure 17 displays the effects of these two parameters. While one parameter was varied, the rest were held constant in the reaction. During the experiments where flow rate was changed, the temperature of the reaction was 250 °C and the ratio of benzene to 1-decene was kept at 4:1. During the experiments where molar ratio was changed, the temperature was also kept at 250 °C and the flow rate was held at 10 mL/g (Figure 17)

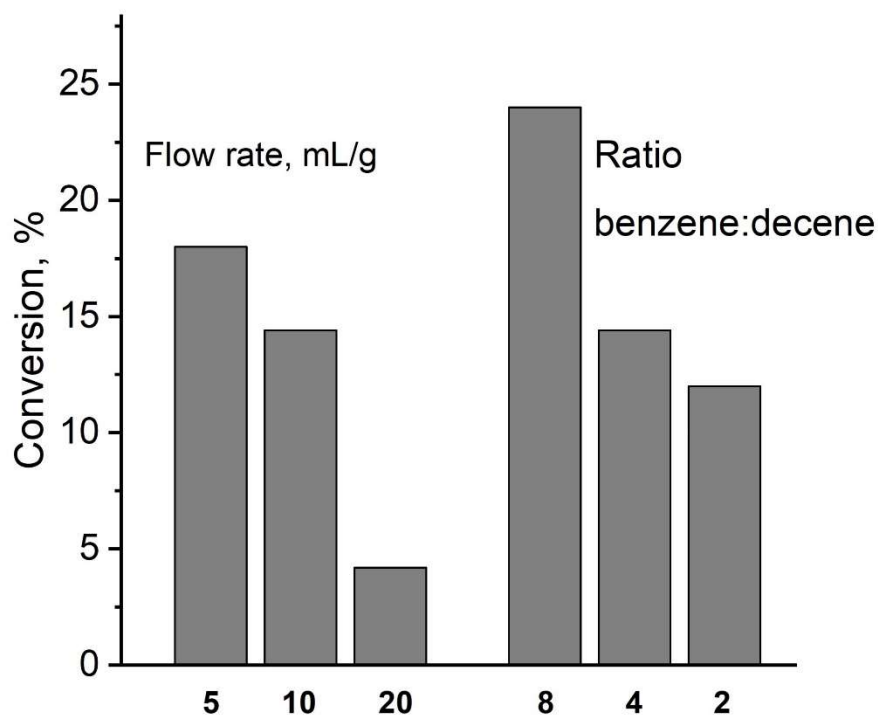


Figure 17. Effects of flow rate (left) and molar ratio (right) on the conversion of 1-decene.

The results of the flow rate variation showed a clear trend where slower flow rates resulted in higher conversions of 1-decene. The highest conversion of 1-decene was observed at the

slowest flow rate of 5 mL/g (Figure 17). On the other hand, the lowest conversion of 1-decene resulted from the fastest flow rate of 20 mL/g. The slower flow rate allowed for more time for interaction between the catalyst and reactants leading to a higher conversion overall.

The varying molar ratio experiments also showed a clear trend where a higher ratio of benzene to 1-decene resulted in a higher conversion. The reaction mixture containing a molar ratio of 8:1 benzene to 1-decene showed the greatest conversion into phenylalkanes while the lowest ratio 2:1 benzene to 1-decene showed a much lower conversion comparatively (Figure 17). This is attributed to the kinetics of the reaction involving an excess of benzene in the mixture allowing for more conversion of the limited reactant 1-decene. Of course, a higher conversion of 1-decene was caused by an equilibrium shift towards the phenylalkane product as the benzene concentration increased.

While temperature of the reaction was varied, the flow rate was held constant at 10 mL/g and the molar ratio was also held constant at 4:1 benzene to 1-decene. The results from the experiments where temperature was varied between 200, 225, and 250 °C are displayed in Figure 18. The results conveyed that a 250 °C (the highest temperature) column temperature produced the highest conversion of 1-decene while the 200 °C column produced the lowest yield. This trend showed that as the temperature increased, the conversion of 1-decene also increased. As such, another set of experiments were completed to examine if the trend held by increasing the temperature to 275 °C. Unfortunately, no phenyldecane product resulted from these experiments due to fast polymerization of decene at such a high temperature. The decene polymerized before alkylation could occur. Thus, 250 °C was determined to be the optimal temperature for the alkylation of benzene with 1-decene (Figure 18).

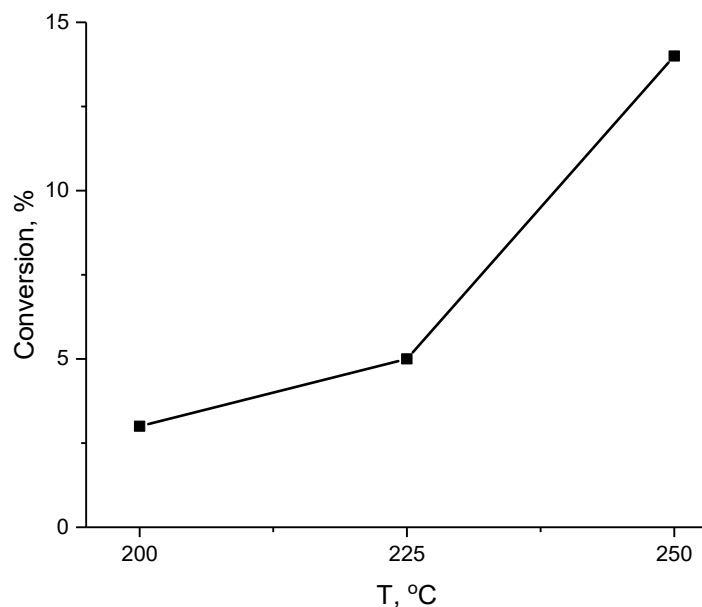


Figure 18. Conversion of 1-decene at various reaction temperatures

### 3.3 Deactivated Catalyst

#### *Chemical Composition*

After catalysis, the PTA-SiO<sub>2</sub>/Al<sub>2</sub>O<sub>3</sub> catalyst darkened in color to black. Chemical analysis of the post reaction catalyst revealed carbon deposition on the surface. Carbon deposition occurs as a result of side reactions at high temperatures involving alkene polymerization and subsequent deposition onto the surface of the catalyst. Carbon deposition may reduce activity of the catalyst. Considerable carbon contents on the PTA-SiO<sub>2</sub>/Al<sub>2</sub>O<sub>3</sub> catalyst was measured with 13.04% by weight.

The FT-IR spectrum of the deactivated catalyst, as shown in Figure 8 (4), displays peaks at 2927 and 2854 cm<sup>-1</sup>. These signals are characteristic of carbon-hydrogen bonds confirming there was deposition on the surface of the catalyst from polymerization of the alkene. Furthermore, the signal around 962 cm<sup>-1</sup> characteristic of the tungsten-oxygen bonds remains unchanged indicating the post reaction catalyst still contained the PTA.

AAS analysis was completed with a tungsten lamp measuring concentration of the tungstate ions to determine PTA content. Fresh catalyst contained 0.027 mmol/g of PTA while the post reaction catalyst had a PTA content of 0.026 mmol/g indicating negligible change in PTA content. Thus, the catalyst experienced no leeching from the support demonstrating that the covalent bonds between the PTA and silica were stable.

### *Physical Characteristics*

The BET surface area of the post reaction PTA-SiO<sub>2</sub>/Al<sub>2</sub>O<sub>3</sub> was measured to have an average value of 176.4 cm<sup>3</sup>/g compared to the fresh catalyst's surface area of 168.3 cm<sup>3</sup>/g (Table 2). The slight increase in surface area is negligible but could show a slight change in physical structure of the catalyst particles. There was also a slight decrease in the average particle size of the spent catalyst with a mean particle size of 787 nm compared to the mean particle size of 856 nm of the fresh catalyst. The slight decrease in average particle size can be accounted to the carbon deposition which causes deagglomeration of particles in the sample. The large agglomerates of the PTA-SiO<sub>2</sub>/Al<sub>2</sub>O<sub>3</sub> catalyst broke into smaller particles since the carbon deposition disrupted the structure.

The PDI also decreased slightly to 0.849 compared to the fresh catalyst PDI of 0.935. The post reaction catalyst was comprised of more similar sized molecules due to the deagglomeration into smaller particles.

Overall, the various analyses display that the PTA-SiO<sub>2</sub>/Al<sub>2</sub>O<sub>3</sub> catalyst's chemical and physical structures were altered due to the carbon deposition that took place during the catalytic reactions. Thus, the deposition will need to be addressed to find the optimal method for regenerating the catalyst for further use in reactions.

## CONCLUSIONS

The overall results of this research displayed that the covalently supported phosphotungstic acid granulated with  $\gamma$ -alumina (PTA-SiO<sub>2</sub>/Al<sub>2</sub>O<sub>3</sub>) had high catalytic activity in the reactions of alkene isomerization and benzene alkylation with 1-decene. Thus, the PTA-SiO<sub>2</sub> shows promise as a useful alternative to harmful homogenous catalysts in industrial alkylation. However, the gas phase alkylation allowed for carbon deposition of polymerized alkene on the surface of the catalyst causing blocking of active sites followed by deactivation. Future work in this area will need to evaluate regeneration methods or test the effectiveness of increasing pressure in the system. Under increased pressure, the reaction may proceed at high temperatures in the liquid phase allowing for optimal alkylation while preventing carbon deposition. On top of this, the liquid phase alkylation in previous projects showed higher activity. Therefore, a focus of future research is to utilize liquid phase alkylation in the flow reactor mechanism since flow reactors are more applicable in industrial processes.

## REFERENCES

- (1) Eganhouse, R. P.; Blumfield, D. L.; Kaplan, I. R. Long-Chain Alkylbenzenes as Molecular Tracers of Domestic Wastes in the Marine Environment. *Environmental Science & Technology* **1983**, *17* (9), 523–530. <https://doi.org/10.1021/es00115a006>.
- (2) Elsgaard, L.; Petersen, S. O.; Deboz, K. Effects and Risk Assessment of Linear Alkylbenzene Sulfonates in Agricultural Soil. 1. Short-Term Effects on Soil Microbiology. *Environmental Toxicology and Chemistry* **2001**, *20* (8), 1656–1663. <https://doi.org/10.1002/etc.5620200806>.
- (3) Mungray, A. K.; Kumar, P. Fate of Linear Alkylbenzene Sulfonates in the Environment: A Review. *International Biodeterioration & Biodegradation* **2009**, *63* (8), 981–987. <https://doi.org/10.1016/j.ibiod.2009.03.012>.
- (4) Perego, C.; Ingallina, P. Recent Advances in the Industrial Alkylation of Aromatics: New Catalysts and New Processes. *Catalysis Today* **2002**, *73* (1-2), 3–22. [https://doi.org/10.1016/S0920-5861\(01\)00511-9](https://doi.org/10.1016/S0920-5861(01)00511-9).
- (5) Scheibel, J. J. The Evolution of Anionic Surfactant Technology to Meet the Requirements of the Laundry Detergent Industry. *Journal of Surfactants and Detergents* **2004**, *7* (4), 319–328. <https://doi.org/10.1007/s11743-004-0317-7>.
- (6) Kocal, J. A.; Vora, B. V.; Imai, T. Production of Linear Alkylbenzenes. *Applied Catalysis A: General* **2001**, *221* (1), 295–301. [https://doi.org/10.1016/S0926-860X\(01\)00808-0](https://doi.org/10.1016/S0926-860X(01)00808-0).
- (7) Bai, S.; Dai, Q.; Chu, X.; Wang, X. Dehydrochlorination of 1,2-Dichloroethane over Ba-Modified Al<sub>2</sub>O<sub>3</sub> Catalysts. *RSC Advances* **2016**, *6* (58), 52564–52574. <https://doi.org/10.1039/c6ra08855d>.
- (8) Jones, E. K. Commercial Alkylation of Paraffins and Aromatics. *Advances in Catalysis* **1958**, 165–195. [https://doi.org/10.1016/S0360-0564\(08\)60407-1](https://doi.org/10.1016/S0360-0564(08)60407-1).
- (9) Reddy, B. M.; Sreekanth, P. M.; Lakshmanan, P. Sulfated Zirconia as an Efficient Catalyst for Organic Synthesis and Transformation Reactions. *Journal of Molecular Catalysis A: Chemical* **2005**, *237* (1), 93–100. <https://doi.org/10.1016/j.molcata.2005.04.039>.
- (10) UOP Linear Alkylbenzene (LAB) Complex. UOP, A Honeywell Company, 2007. <https://www.honeywell-uop.cn/wp-content/uploads/2011/02/UOP-LAB-Complex-DataSheet.pdf>
- (11) Sartori, G.; Ballini, R.; Bigi, F.; Bosica, G.; Maggi, R.; Righi, P. Protection (and Deprotection) of Functional Groups in Organic Synthesis by Heterogeneous Catalysis. *Chemical Reviews* **2003**, *104* (1), 199–250. <https://doi.org/10.1021/cr0200769>.
- (12) Wilson, K.; Clark, J. H. Solid Acids and Their Use as Environmentally Friendly Catalysts in Organic Synthesis. *Pure and Applied Chemistry* **2000**, *72* (7), 1313–1319. <https://doi.org/10.1351/pac200072071313>.
- (13) Nikoonahad, A.; Djahed, B.; Norzaee, S.; Eslami, H.; Derakhshan, Z.; Miri, M.; Fakhri, Y.; Hoseinzadeh, E.; Ghasemi, S. M.; Balarak, D.; Fallahzadeh, R. A.; Zarrabi, M.;

- Taghavi, M. An Overview Report on the Application of Heteropoly Acids on Supporting Materials in the Photocatalytic Degradation of Organic Pollutants from Aqueous Solutions. *PeerJ* **2018**, *6*, e5501. <https://doi.org/10.7717/peerj.5501>.
- (14) de Almeida, J. L. G.; Dufaux, M.; Taarit, Y. B.; Naccache, C. Linear Alkylbenzene. *Journal of the American Oil Chemists' Society* **1994**, *71* (7), 675–694. <https://doi.org/10.1007/bf02541423>.
- (15) Zhang, Z.; Han, Y.; Zhu, L.; Wang, R.; Yu, Y.; Qiu, S.; Zhao, D.; Xiao, F.-S. Strongly Acidic and High-Temperature Hydrothermally Stable Mesoporous Aluminosilicates with Ordered Hexagonal Structure. *Angewandte Chemie* **2002**, *114* (13), 2331–2331. <https://doi.org/10.1002/ange.200200703>.
- (16) Nowak, I.; Ziolk, M. Niobium Compounds: Preparation, Characterization, and Application in Heterogeneous Catalysis. *Chemical Reviews* **1999**, *99* (12), 3603–3624. <https://doi.org/10.1021/cr9800208>.
- (17) Tejero, B.; Danvilla, M. Alkylation of Aromatic Hydrocarbons in Fixed Bed Catalytic Process. EP 0353813B1, December 13, 1995.
- (18) Borutskii, P. N.; Kozlova, E. G.; Podkletnova, N. M.; Gil'chenok, N. D.; Sokolov, B. G.; Zuev, V. A.; Shatovkin, A. A. Alkylation of Benzene with Higher Olefins on Heterogeneous Catalysts. *Petroleum Chemistry* **2007**, *47* (4), 250–261. <https://doi.org/10.1134/s0965544107040044>.
- (19) Young, L. Preparing Phenylalkanes. US 4301316-A, November 17, 1981.
- (20) Vázquez, P.; Pizzio, L.; Romanelli, G.; Autino, J.; Cáceres, C.; Blanco, M. Mo and W Heteropolyacid Based Catalysts Applied to the Preparation of Flavones and Substituted Chromones by Cyclocondensation of O-Hydroxyphenyl Aryl 1,3-Propanediones. *Applied Catalysis A: General* **2002**, *235* (1-2), 233–240. [https://doi.org/10.1016/s0926-860x\(02\)00266-1](https://doi.org/10.1016/s0926-860x(02)00266-1).
- (21) Kozhevnikov, I. V. Heteropoly Acids and Related Compounds as Catalysts for Fine Chemical Synthesis. *Catalysis Reviews* **1995**, *37* (2), 311–352. <https://doi.org/10.1080/01614949508007097>.
- (22) Wen, S.; Guan, W.; Wang, J.; Lang, Z.; Yan, L.; Su, Z. Theoretical Investigation of Structural and Electronic Properties of  $[PW_{12}O_{40}]^{3-}$  on Graphene Layer. *Dalton Transactions* **2012**, *41* (15), 4602. <https://doi.org/10.1039/c2dt12465c>.
- (23) Supported Phosphotungstic Acid Catalyst Preparation. <http://news.chinatungsten.com/en/tungsten-information/109314-ti-15487>.
- (24) Kozhevnikov, I. V. Catalysis by Heteropoly Acids and Multicomponent Polyoxometalates in Liquid-Phase Reactions. *Chemical Reviews* **1998**, *98* (1), 171–198. <https://doi.org/10.1021/cr960400y>.
- (25) Briand, L. E.; Baronetti, G. T.; Thomas, H. J. The State of the Art on Wells–Dawson Heteropoly-Compounds. *Applied Catalysis A: General* **2003**, *256* (1-2), 37–50. [https://doi.org/10.1016/s0926-860x\(03\)00387-9](https://doi.org/10.1016/s0926-860x(03)00387-9).

- (26) Romanelli, G.; Autino, J. Recent Applications of Heteropolyacids and Related Compounds in Heterocycles Synthesis. *Mini-Reviews in Organic Chemistry* **2009**, *6* (4), 359–366. <https://doi.org/10.2174/157019309789371578>.
- (27) Zhu, H.-O.; Ren, X.-Q.; Wang, J. A Comparative Study of the Catalytic Behavior of SBA-15 Supported Heteropoly Acid  $H_3PW_{12}O_{40}$  and H-Y Catalysts in the Alkylation of Benzene with 1-Dodecene. *Reaction Kinetics and Catalysis Letters* **2004**, *83* (1), 19–24. <https://doi.org/10.1023/b:reac.0000037371.31835.60>.
- (28) Faghihian, H.; Mohammadi, M. H. A Novel Catalyst for Alkylation of Benzene. *Comptes Rendus Chimie* **2012**, *15* (11-12), 962–968. <https://doi.org/10.1016/j.crci.2012.08.007>.
- (29) Li, K.; Hu, J.; Li, W.; Ma, F.; Xu, L.; Guo, Y. Design of Mesoporous  $H_3PW_{12}O_{40}$ -Silica Materials with Controllable Ordered and Disordered Pore Geometries and Their Application for the Synthesis of Diphenolic Acid. *Journal of Materials Chemistry* **2009**, *19* (45), 8628. <https://doi.org/10.1039/b910416j>.
- (30) Yang, L.; Qi, Y.; Yuan, X.; Shen, J.; Kim, J. Direct Synthesis, Characterization and Catalytic Application of SBA-15 Containing Heteropolyacid  $H_3PW_{12}O_{40}$ . *Journal of Molecular Catalysis A: Chemical* **2005**, *229* (1-2), 199–205. <https://doi.org/10.1016/j.molcata.2004.11.024>.
- (31) Dufaud, V.; Lefebvre, F. Inorganic Hybrid Materials with Encapsulated Polyoxometalates. *Materials* **2010**, *3* (1), 682–703. <https://doi.org/10.3390/ma3010682>.
- (32) Rafiee, E.; Shahbazi, F. One-Pot Synthesis of Dihydropyrimidones Using Silica-Supported Heteropoly Acid as an Efficient and Reusable Catalyst: Improved Protocol Conditions for the Biginelli Reaction. *Journal of Molecular Catalysis A: Chemical* **2006**, *250* (1-2), 57–61. <https://doi.org/10.1016/j.molcata.2006.01.049>.
- (33) Kumar, G. S.; Vishnuvarthan, M.; Palanichamy, M.; Murugesan, V. SBA-15 Supported HPW: Effective Catalytic Performance in the Alkylation of Phenol. *Journal of Molecular Catalysis A: Chemical* **2006**, *260* (1-2), 49–55. <https://doi.org/10.1016/j.molcata.2006.07.050>.
- (34) Liu, Y.; Xu, L.; Xu, B.; Li, Z.; Jia, L.; Guo, W. Toluene Alkylation with 1-Octene over Supported Heteropoly Acids on MCM-41 Catalysts. *Journal of Molecular Catalysis A: Chemical* **2009**, *297* (2), 86–92. <https://doi.org/10.1016/j.molcata.2008.09.007>.
- (35) Guo, Y.; Li, K.; Yu, X.; Clark, J. H. Mesoporous  $H_3PW_{12}O_{40}$ -Silica Composite: Efficient and Reusable Solid Acid Catalyst for the Synthesis of Diphenolic Acid from Levulinic Acid. *Applied Catalysis B: Environmental* **2008**, *81* (3-4), 182–191. <https://doi.org/10.1016/j.apcatb.2007.12.020>.
- (36) Kankam, Kofi, "Alkylation of Benzene on Immobilized Phosphotungstic Acid" (2020). Electronic Theses and Dissertations. Paper 3847. <https://dc.etsu.edu/etd/3847>
- (37) Kuvayskaya, Anastasia, "Immobilization of Phosphotungstic Acid on Silica Surface for Catalytic Alkylation of Aromatic Compounds" (2020). Electronic Theses and Dissertations. Paper 3738. <https://dc.etsu.edu/etd/3738>



- (38) Kuvayskaya, A.; Mohseni, R.; Vasiliev, A. Alkylation of Benzene by Long-Chain Alkenes on Immobilized Phosphotungstic Acid. *Journal of Porous Materials* **2022**. <https://doi.org/10.1007/s10934-022-01202-8>.
- (39) Seaton, K.; Little, I.; Tate, C.; Mohseni, R.; Roginskaya, M.; Povazhniy, V.; Vasiliev, A. Adsorption of Cesium on Silica Gel Containing Embedded Phosphotungstic Acid. *Microporous and Mesoporous Materials* **2017**, *244*, 55–66. <https://doi.org/10.1016/j.micromeso.2017.02.025>.
- (40) Hosseini, S. A.; Niaei, A.; Salari, D. Production of  $\gamma$ -Al<sub>2</sub>O<sub>3</sub> from Kaolin. *Open Journal of Physical Chemistry* **2011**, *01* (02), 23–27. <https://doi.org/10.4236/ojpc.2011.12004>.